The Photogrammetric Record 20(112): 335–350 (December 2005)

MAPPING SMALL AREAS USING A LOW-COST CLOSE RANGE PHOTOGRAMMETRIC SOFTWARE PACKAGE WITH AERIAL PHOTOGRAPHY

Manuel A. Aguilar (maguilar@ual.es)

Fernando J. Aguilar (faguilar@ual.es)

Francisco Agüera (faguera@ual.es)
University of Almería, Spain

Abstract

Generating maps of small areas using conventional aerial photography is of great interest for small engineering firms. The main problem is the high cost of the sophisticated digital photogrammetric workstations usually employed. In this paper, a low-cost close range photogrammetric software package is used to measure the three-dimensional coordinates of points on the land surface from a photogrammetric flight at a scale of approximately 1:5000. Furthermore, the influence of the type of scanner used to digitise photographs (consumer-grade or photogrammetric scanner), the resolution of the digital images and the number of control points required are examined. The root mean square errors obtained at the check points, using a low-cost close range software package, scanning aerial images with a photogrammetric scanner and 24 ground control points, were around 116 mm for X and Y coordinates, and 191 mm for Z. These levels of accuracy allow the generation of planimetric maps at a scale of 1:1500 and topographic maps with a contour interval of around 1 m. When the images were scanned with a consumer-grade scanner, the root mean square errors were around 150 mm for X and Y, and 271 mm for Z.

Keywords: aerial photography, close range photogrammetry, land surveys, mapping small areas, topographic mapping

Introduction

Classical photogrammetry, based on mechanical and optical–mechanical solutions, has been giving way in the past few years to digital photogrammetry. The most remarkable aspect of the present digital era is the highly sophisticated digital photogrammetric workstation (DPW), with which the automation of many of the photogrammetric flowline processes (interior orientation, exterior orientation, aerial triangulation, automatic digital elevation model (DEM) generation and digital orthorectification) can be achieved. With the advent of suitable computing processors this now allows high rates of data capture (Baily et al., 2003). Likewise, high accuracy and reliability of the data generated using digital photogrammetric techniques have been reported (Walker, 1995; Smith and Smith, 1996; Gooch et al., 1999). The only disadvantage of these photogrammetric software packages, among which SOCET SET from

Blackwell Publishing Ltd. 9600 Garsington Road, Oxford OX4 2DQ, UK and 350 Main Street Malden, MA 02148, USA.

LH Systems and ImageStation SSK Z/I Imaging from Intergraph can be included, is their high cost which places them out of the reach of small engineering firms that do not specialise in generating maps.

On the other hand, close range photogrammetry offers the possibility of obtaining the three-dimensional (3D) coordinates of an object from two-dimensional (2D) digital images in a rapid, accurate, reliable, flexible and economical way. This makes it an ideal tool for precise industrial measurement (Fraser, 1993). Close range photogrammetric systems (CRPS) have been used successfully in recent times for measurements in fluid physics experiments in space (Maas et al., 2002), underwater archaeological surveying (Green et al., 2002), monitoring the thermal deformation of steel beams (Fraser and Riedel, 2000), for mapping low relief fluvial geomorphic features ranging from 10 to 100 m^2 (Heritage et al., 1998), for the survey of a historic building (Mills and Barber, 2004) and for the modelling of mouldboard plough surfaces (Aguilar et al., 2005). These close range and low-cost digital software packages such as Photomodeler (Eos Systems Inc., Vancouver, Canada) and ShapeCapture (ShapeQuest Inc., Nepean, Canada) cost about 5% of the price of a DPW.

Most planimetric or topographic maps are produced from aerial photography and stereo photogrammetry. To map large areas, the use of a DPW is almost essential. However, if the area to be mapped is local, small-format (35 mm film or digital cameras) aerial photography is seen as a low-cost alternative to classic and expensive large-format (230 mm × 230 mm) photography (Fraser, 1994; Mills et al., 1996; Mason et al., 1997). Nevertheless, some photogrammetric flights carried out by government agencies that produce detailed national or regional maps are available for sale at low prices. In the case of Andalusia (southern Spain), photography at scales of 1:60 000 and 1:20 000 is available for the whole of the region, while large scales (1:3000 or 1:5000) are available for urban areas only. These flights were commissioned by the government of Andalusia between 1984 and 2001, and the price per paper print is about €3.

Owing to the need to reduce costs in aerial photogrammetry so that small engineering firms can produce their own maps for small areas, the following objectives are examined in this paper:

(1) Evaluate the accuracy in measuring the 3D coordinates of points on the land surface using a low-cost close range photogrammetric software package (developed for convergent photographic networks in which exposures are made at small distances from the object) working with conventional aerial photography at an approximate scale of 1:5000 and a flying height above mean ground level of around 760 m.
(2) Study of the loss of accuracy due to using a consumer-grade scanner vs. a photogrammetric scanner for the scanning of aerial photographs.
(3) Comparison of the accuracy in measuring the 3D coordinates of the ground points obtained using low-cost photogrammetric methods and produced by a DPW working under the same conditions.

METHODOLOGY

Original Image Data Acquisition

The colour photographs used in this study belong to a photogrammetric flight at an approximate scale of 1:5000 with 60% and 25% longitudinal and transversal overlap, respectively. It was commissioned by the State-owned Company for the Agrarian and Fishing Development of Andalusia (D.a.p.) and carried out on 15th May 2001, covering an area of

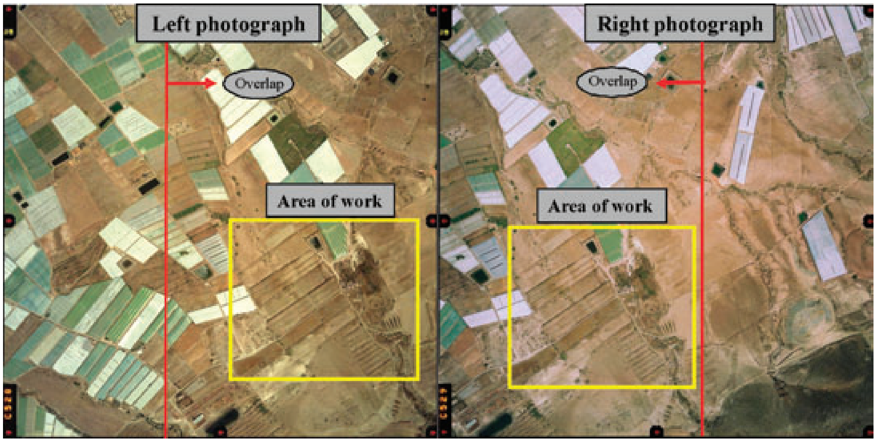

FIG. 1. Left and right photographs and work area.
This figure appears in colour in the electronic version of the article and in the plate section at the front of the printed journal

around 160 km^2 in Almería, Spain. The camera used was an RMK TOP 15 with a wide-angle lens (focal length $f = 153{\cdot}33$ mm) and the film chosen was AGFA AVIPHOT H100. Full details of camera calibration data were supplied. For this study a stereopair of this flight comprising photographs 528 (left) and 529 (right) was selected (Fig. 1).

Photo Scanning

Photographs 528 (left) and 529 (right) selected for this study had to be scanned to create digital files before they could be imported into the two photogrammetric systems compared in this paper (low-cost CRPS and DPW).

The photographs were scanned using a Vexcel UltraScan 5000 photogrammetric scanner at a geometric resolution of 20 µm per pixel (~1270 dpi) and a colour depth of 24 bits (true colour). The digital images were stored in TIFF format, each image taking up approximately 392 Mb (Table I). A description and evaluation of the UltraScan 5000 photogrammetric scanner were given by Gruber and Leberl (2001).

The photos were also scanned using a mid-priced HP Scanjet 5400C scanner with different resolutions in order to study the effect of the use of a non-calibrated consumer-grade scanner on the accuracy reached with the close range photogrammetric software package

TABLE I. Photogrammetric projects tested.

Project	*Scanner*	*Image*	*Resolution (µm)*	*File size TIFF (Mb)*	*Ground pixel size (m)*	*Photogrammetric system*
ZI	Vexcel 5000	Full	20	392	0·10	DPW
CR_0	Vexcel 5000	Split	20	65·1	0·10	CRPS
CR_1	HP 5400C	Split	20	65·1	0·10	CRPS
CR_2	HP 5400C	Split	24	44·5	0·12	CRPS
CR_3	HP 5400C	Split	28	32·7	0·14	CRPS
CR_4	HP 5400C	Split	34	22·7	0·17	CRPS
CR_5	HP 5400C	Split	42	14·5	0·21	CRPS

DPW = digital photogrammetric workstation; CRPS = close range photogrammetric system.

(Table I). This flatbed scanner had an optical resolution of 2400 × 2400 dpi and a 48-bit depth maximum colour sample. The original photographs were digitised in TIFF format and 24 bits.

The images scanned with the consumer-grade HP Scanjet were only used in the projects carried out with the CRPS, whilst those generated with the Vexcel UltraScan 5000 photogrammetric scanner were imported into both the CRPS and the DPW photogrammetric system (Table I). The work area was reduced to approximately 500 m × 450 m (Fig. 1) which occupied 25% of the overlapping surface of the stereopair. The limitation of the work area was due to the impossibility of scanning the whole area of each photo (230 mm × 230 mm) with the A4 format of the HP Scanjet scanner and to the problems of the CRPS used in this study to load and handle files over 250 Mb. Therefore, all the digital images imported by the CRPS were split beforehand, and only information from the work area was included.

Ground Control and Check Points

Within the work area, 93 randomly distributed ground points were selected. These points were located on well-defined natural and man-made features in both digital images (such as corners of irrigation outlet boxes, greenhouses, irrigation conduits, bushes and rocks). Differential global positioning system (DGPS) observations were used to measure ground points. This method offered sufficient accuracy (precision of ±10 mm + 1 ppm over distances of 15 km) and did not require direct lines of sight. The points were recorded using a Trimble GPS 4800 total station working in real-time kinematic mode (RTK). The RTK survey to measure the 93 ground points was based on four ground control points belonging to the campaign carried out to control the whole area flown (160 km^2).

Of a total of 93 GPS points collected, 57 were retained as check points in order to compare the photogrammetrically extracted data coordinates with the corresponding ground survey values. The remaining 36 points were used to carry out eight different control point repetitions (four combinations of 12 control points and four of 24) used in the two photogrammetric systems tested in this study.

Close Range Photogrammetric System

A Windows-based, low-cost digital close range photogrammetric software package named ShapeCapture (version 4.0) (http://www.shapecapture.com) that allows the extraction of 3D information from overlapping photographs in monoscopic mode was used to obtain the coordinates for the 57 check points in the work area. This software has three integrated modules: calibration, registration and computation of 3D coordinates.

The objective of the calibration is to solve the exterior and interior parameters of the camera using known photogrammetric ground control points in the field of view. The interior parameters are focal length (f), X and Y coordinates of the principal point of the image (x_0, y_0), affine image parameters to correct for scale difference and non-perpendicularity of the X and Y image coordinates (A, B), radial lens distortion parameters (k_1, k_2) and decentring lens distortion parameters (p_1, p_2). The exterior parameters are the position and orientation of the camera when the image was taken. These are the coordinates of the camera projection centre (X_c, Y_c, Z_c) and three rotation angles around the X (pitch or ω), Y (roll or ϕ) and Z (yaw or κ) axes.

Once the photographs had been calibrated, the image coordinates of the check points were pointed on the natural features, in each of the two images. The following step was the registration to determine the position and orientation of each image relative to the reference coordinate system. Registration is based on a photogrammetric bundle adjustment (Kenefick et al., 1972; Granshaw, 1980), which uses the least squares estimation procedure to derive the best estimates for the positions and orientations of each frame. This procedure gives the 3D coordinates of all the points used for registration.

Photographs used with this photogrammetric system were split according to the work area and scanned both with a photogrammetric scanner and with a consumer-grade scanner at various different resolutions (Table I).

Digital Photogrammetric Workstation

Within the variety of choice among the photogrammetric systems currently available, the sophisticated DPWs stand out without any doubt. The Z/I Imaging SSK ImageStation from Intergraph, mounted upon a Dell Precision 530 MT WorkStation, has been used in this study as an example of a sophisticated photogrammetric system, which is becoming a standard component of important mapping organisations in the private and public sectors.

Once photographs 528 and 529 have been scanned with the Vexcel UltraScan 5000 photogrammetric scanner, images can be imported into the system where the interior orientation is performed using camera calibration data and the locations of fiducial marks. The next step is the exterior orientation of the images. This process, known as triangulation, registers the images to the ground and to other images. In the SSK ImageStation system, this process can be performed automatically using ImageStation Automatic Triangulation (ISAT). Aerial triangulation allows the calculation of the exterior orientation parameters of all the photos that compose a photogrammetric block from a minimal number of ground control points. The steps followed by the majority of DPWs are: semi-automatic measurement of ground control points, generation of tie and pass points by stereo autocorrelation, calculation of the photogrammetric block using bundle adjustment and transfer of the resulting exterior orientation parameters of each photograph.

Statistical Analysis

In the case of CRPS, the calibration process requires eight or more control points with known coordinates. In the present case, with the 36 ground control points available, four repetitions were carried out using sets of 12 and 24 points. Many points were included in more than one repetition, though the combinations from them were always different. For a good distribution of the ground control points selected in each repetition, the work area was divided into 12 plots of $125\,\text{m} \times 112{\cdot}5\,\text{m}$ each, organised in four rows and three columns. The distribution of control and check points within the work area can be seen in Fig. 2.

Each repetition of the 12 control points had one point in each of the plots, whilst the repetitions of the 24 points had two. Bearing in mind the factorial design followed, the CRPS was used for six different digital images (Table I), 12 or 24 control points for calibration and four repetitions, thus, the final total number of photogrammetric projects carried out with the CRPS was 48.

The DPW was used only with the full image obtained with the photogrammetric scanner. The same data-sets of 12 and 24 control points used previously were employed, so that taking into account the four repetitions, eight different photogrammetric projects were carried out.

In each of these projects the 3D coordinates of each of the 57 check points were calculated and compared with the coordinates measured with DGPS. A few outliers (check points where errors were larger than expected for the normal error distribution) were eliminated. Outliers were defined as errors larger than three times the standard deviation of a data-set (3σ) (Daniel

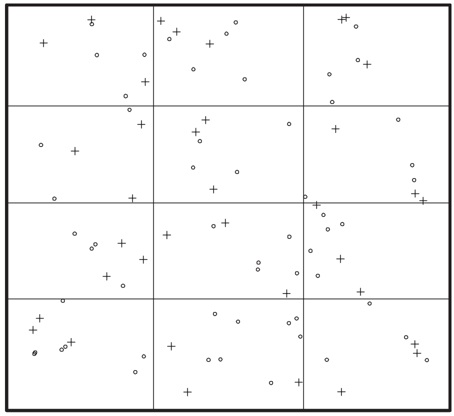

FIG. 2. Distribution of check (circles) and control (cross) points in the work area.

and Tennant, 2001). After this, the root mean square errors (rmse) for *X*, *Y*, *Z* (equations (1), (2) and (3)) were computed by

$$rmse_x = \sqrt{\frac{1}{n}\sum_{i=1}^{n}(X_{iDGPS} - X_{iPS})^2} \quad (1)$$

$$rmse_y = \sqrt{\frac{1}{n}\sum_{i=1}^{n}(Y_{iDGPS} - Y_{iPS})^2} \quad (2)$$

$$rmse_z = \sqrt{\frac{1}{n}\sum_{i=1}^{n}(Z_{iDGPS} - Z_{iPS})^2} \quad (3)$$

where n is the number of check points; (X_{iDGPS}, Y_{iDGPS}, Z_{iDGPS}) are the check point coordinates measured with DGPS and (X_{iPS}, Y_{iPS}, Z_{iPS}) are the ones obtained with a photogrammetric system.

When the spatial data-sets obtained with the different photogrammetric projects are used for mapping an area, it is necessary to calculate their vertical and horizontal accuracy. Thus, the scale and contour interval of the map can be estimated.

If systematic errors have been eliminated, error is normally distributed and independent in each component, the horizontal and vertical accuracy values at 95% confidence level, ($Accuracy_r$ and $Accuracy_z$) according to the US National Standard for Spatial Data Accuracy (NSSDA) (FGDC, 1998), can be computed by

$$Accuracy_r = 1{\cdot}7308 \times rmse_r \quad (4)$$

$$Accuracy_z = 1{\cdot}9600 \times rmse_z \quad (5)$$

where $rmse_r$ is the horizontal (radial) root mean square error given as

$$rmse_r = \sqrt{rmse_x^2 + rmse_y^2}. \quad (6)$$

Bearing in mind that the visual perception limit of the human eye is 0·2 mm, the largest scale to represent the set of spatial data in a map will be computed by

$$Scale \geq Accuracy_r/0{\cdot}2 \tag{7}$$

where horizontal accuracy is expressed in millimetres and scale denotes the denominator of the scale.

The minimum possible contour interval (*CI*) according to NSSDA will be computed by

$$CI \geq 3{\cdot}2898 \times rmse_z. \tag{8}$$

As a preliminary step to the above equations, the Kolmogorov–Smirnov test was used to verify that the different data-sets fitted a normal distribution.

Vertical root mean square error ($rmse_z$), horizontal (radial) root mean square error ($rmse_r$) (equation (4)), and the maximum errors indicated by the planimetric and altimetric residuals ($Emax_r$, $Emax_z$) were the variables observed in the analysis of variance for the designed factorial model with four repetitions (Snedecor and Cochran, 1980). The sources of variation analysed were the number of control points that participated in the creation of the photogrammetric project, the seven types of photogrammetric project tested (Table I) and the interaction between them. When the results of the variance analysis were significant the separation of means was carried out using Duncan's multiple range test with a 95% confidence level.

Principal Point Location

The aim of this section was to verify that the close range photogrammetry package used did not treat the split image as a whole photograph, but as part of one. Thus, the geometric position of the principal point calculated in a photogrammetric project carried out from two full images should be the same as that obtained in a project generated from two split images. However, this position would be represented by different coordinates (x_0, y_0) since the origin of the coordinate system, situated at all times in the upper left hand corner of the images that participated in the photogrammetric project, varied depending on whether the images were full or split (Fig. 3).

The full images used in the first photogrammetric project of this trial were scanned with a Vexcel UltraScan 5000 photogrammetric scanner, although their resolution was transformed

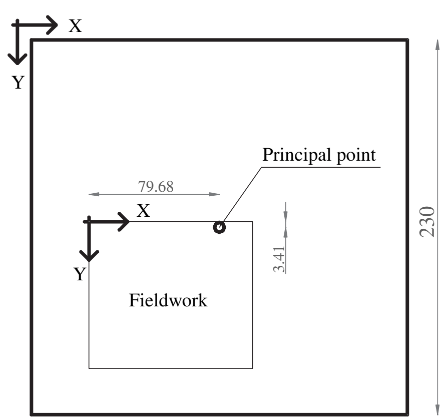

FIG. 3. Expected principal point position in the right photograph and *X*, *Y* coordinates (mm) in the split image coordinate system whose origin is located at the upper left corner of the split photograph (work area).

into a resolution of 600 dpi (~42 μm per pixel) by means of a bicubic resample. These images were split according to the work area to undertake the second photogrammetric project. Both projects were carried out with the CRPS using 12 control points and three repetitions.

RESULTS AND DISCUSSION

The Use of Split Photographs

Fig. 3 shows how the expected location of the principal point in the right-hand photograph of the photogrammetric projects carried out with full images is approximately in the geometric centre of the photo, the side of which measures 230 mm. Thus, the coordinates of the principal point should be in this case approximately 115 mm, both for x_0 and for y_0. When photogrammetric projects are carried out using split images, the coordinates of the principal point for the right-hand photograph would be around 79 mm for x_0 and 3·5 mm for y_0, if the CRPS computes the projects in the understanding that the split images are part of full images. In the case of the CRPS computing the projects and considering split images as full ones, the principal point coordinates should be around 50 mm in x_0 and 45 mm in y_0.

The principal point coordinates for those projects carried out using CRPS for full and split images are shown in Table II. These results show that the CRPS does in fact compute split images with the understanding that they are part of a larger image, so there is no objection to using them. On the other hand, the same table shows the standard deviations of the principal point coordinates calculated in the different projects carried out with full and split images, these having similar values in both types of photogrammetric projects.

Orientation Parameters

Table III shows how the standard deviations of the exterior orientation parameters in the right and left photographs of projects ZI and CR_0 decrease when the number of control points increases, although this reduction is greater using the CRPS. In any case, the standard deviations for CRPS are greater than those obtained with DPW for any number of control points used. This shows that the ZI system is stronger for the calculation of the external orientation parameters than the CRPS system. On the other hand, the internal orientation parameters used in the DPW are the data from the calibration report of the camera, so that the accuracy of these data has been contrasted. The CRPS only introduces the focal distance as a fixed parameter for internal orientation, whilst the rest are calculated from the ground control points using digital camera self-calibration (Fraser, 1997).

TABLE II. Mean and standard deviation of the principal point location after right photograph calibration with CRPS and 12 control points using full and split imagery at 600 dpi geometric resolution.

Principal point	*Full imagery*		*Split imagery*	
	Mean (mm)	*Standard deviation (mm)*	*Mean (mm)*	*Standard deviation (mm)*
x_0	113·1	3·0	77·8	2·7
y_0	116·6	10·0	5·6	5·3

TABLE III. Standard deviation of exterior orientation (EO) parameters of the photographs for photogrammetric projects ZI and CR_0 using 12 and 24 ground control points (GCPs).

EO parameters	*Standard deviation*			
	Left photograph		*Right photograph*	
	12 GCPs	*24 GCPs*	*12 GCPs*	*24 GCPs*
ZI projects				
X_c (mm)	84	53	92	55
Y_c (mm)	111	12	64	64
Z_c (mm)	147	86	133	73
ω (rad)	87×10^{-6}	630×10^{-6}	87×10^{-6}	40×10^{-6}
ϕ (rad)	89×10^{-6}	353×10^{-6}	105×10^{-6}	42×10^{-6}
κ (rad)	93×10^{-6}	54×10^{-6}	89×10^{-6}	40×10^{-6}
CR_0 projects				
X_c (mm)	49 810	18 938	17 838	10 145
Y_c (mm)	31 430	11 199	35 178	6594
Z_c (mm)	2625	796	640	325
ω (rad)	4983×10^{-6}	2505×10^{-6}	2948×10^{-6}	2421×10^{-6}
ϕ (rad)	3485×10^{-6}	1443×10^{-6}	1511×10^{-6}	422×10^{-6}
κ (rad)	3313×10^{-6}	1070×10^{-6}	1543×10^{-6}	522×10^{-6}

Planimetric and Altimetric Accuracy

With regard to the planimetric (Table IV) and altimetric errors (Table V) generated in the different photogrammetric projects carried out, they show how the photogrammetric projects using the DPW present significantly lower $rmse_r$ and $rmse_z$ ($p < 0{\cdot}05$) than those with CRPS.

The influence of the number of control points is much more pronounced in CRPS than in DPW, the latter being practically negligible. Although no significant differences are observed in any of the photogrammetric projects tested ($p < 0{\cdot}05$) due to the number of control points, there is a reduction in the variability of the repetitions in CRPS when 24 control points are used which makes it possible to have a stronger separation of the means. This is, without doubt, directly related to the lower variation of the calibration parameters in CRPS with 24 control points as shows in Table III.

The $rmse_r$ presented in Table IV are graded in the following way: the lowest $rmse_r$ occurs in ZI projects, the next one up in CR_0 projects, and the last one, in those projects

TABLE IV. Comparison of mean values of $rmse_r$, $Accuracy_r$ and scale denominator by photogrammetric project obtained with 12 and 24 ground control points (GCPs). Within each column, no significant difference was found between values marked by the same letter *a*, *b*, *c* or *d*, while significant differences at the $p < 0{\cdot}05$ level are indicated between pairs of values with no letters in common.

Projects	*$Rmse_r$ (mm)*		*$Accuracy_r$ (mm)*		*Scale denominator*	
	12 GCPs	*24 GCPs*	*12 GCPs*	*24 GCPs*	*12 GCPs*	*24 GCPs*
ZI	108·6 *a*	105·8 *a*	187·4 *a*	182·9 *a*	937 *a*	915 *a*
CR_0	185·7 *ab*	164·4 *b*	318·4 *ab*	283·2 *b*	1592 *ab*	1416 *b*
CR_1	256·6 *bc*	212·4 *c*	440·1 *bc*	366·9 *c*	2201 *bc*	1835 *c*
CR_2	246·9 *bc*	208·8 *c*	423·3 *bc*	360·0 *c*	2117 *bc*	1800 *c*
CR_3	247·4 *bc*	210·1 *c*	425·9 *bc*	362·8 *c*	2130 *bc*	1814 *c*
CR_4	246·3 *bc*	221·4 *c*	422·2 *bc*	380·6 *c*	2111 *bc*	1903 *c*
CR_5	320·8 *c*	257·1 *d*	530·3 *c*	432·7 *d*	2652 *c*	2164 *d*

TABLE V. Comparison of mean values of $rmse_z$, $Accuracy_z$ and contour interval by photogrammetric project obtained with 12 and 24 ground control points (GCPs). Within each column, no significant difference was found between values marked by the same letter *a*, *b* or *c*, while significant differences at the $p < 0{\cdot}05$ level are indicated between pairs of values with no letters in common.

Projects	*Rmse$_z$ (mm)*		*Accuracy$_z$ (mm)*		*Contour interval (mm)*	
	12 GCPs	*24 GCPs*	*12 GCPs*	*24 GCPs*	*12 GCPs*	*24 GCPs*
ZI	74·7 *a*	71·6 *a*	146·4 *a*	140·4 *a*	246 *a*	236 *a*
CR_0	243·9 *ab*	191·3 *b*	478·1 *ab*	374·9 *b*	802 *ab*	629 *b*
CR_1	360·5 *b*	271·4 *c*	706·6 *b*	532·0 *c*	1186 *b*	893 *c*
CR_2	335·1 *b*	268·1 *c*	656·9 *b*	525·6 *c*	1093 *b*	882 *c*
CR_3	331·5 *b*	275·3 *c*	649·8 *b*	539·6 *c*	1091 *b*	906 *c*
CR_4	367·4 *b*	317·7 *c*	720·2 *b*	622·7 *c*	1209 *b*	1045 *c*
CR_5	447·2 *b*	320·4 *c*	876·5 *b*	628·0 *c*	1471 *b*	1054 *c*

TABLE VI. Comparison of the horizontal and vertical mean maximum errors ($Emax_r$ and $Emax_z$) by photogrammetric project obtained with 12 and 24 ground control points (GCPs). Within each column, no significant difference was found between values marked by the same letter *a*, *b*, *c* or *d*, while significant differences at the $p < 0{\cdot}05$ level are indicated between pairs of values with no letters in common.

Projects	*Emax$_r$ (mm)*		*Emax$_z$ (mm)*	
	12 GCPs	*24 GCPs*	*12 GCPs*	*24 GCPs*
ZI	270·4 *a*	267·9 *a*	197·3 *a*	186·5 *a*
CR_0	447·6 *ab*	493·3 *b*	640·6 *ab*	527·6 *b*
CR_1	622·1 *abc*	540·6 *b*	867·5 *bc*	647·3 *bc*
CR_2	609·4 *abc*	542·2 *b*	745·8 *bc*	653·1 *bc*
CR_3	704·5 *bc*	600·6 *bc*	908·2 *bc*	670·7 *bc*
CR_4	630·3 *bc*	616·6 *bc*	970·6 *bc*	908·6 *d*
CR_5	865·5 *c*	736·4 *c*	1182·7 *c*	879·6 *cd*

carried out with CRPS and with images scanned with the HP Scanjet 5400C consumer-grade scanner with different resolutions. Within the last group of projects, only CR_5 is statistically different from the rest for 24 control points. According to the NSSDA, the horizontal accuracy at the 95% confidence level increases from 182·9 mm for ZI to 432·7 mm for CR_5, using 24 control points.

The behaviour of the $rmse_z$ (Table V) is very similar to that of the $rmse_r$, although the differences between ZI and CR_0 are more apparent. Vertical accuracy at the 95% confidence level (FGDC, 1998) varies between 140·4 mm for ZI and 628 mm for CR_5 for 24 control points. These vertical errors would allow the production of topographic maps with a contour interval of 0·25 m for ZI and of 1 m for CR_0, CR_1, CR_2 and CR_3.

The vertical and planimetric *Emax* obtained in the different photogrammetric projects (Table VI) follow the tendencies discussed for $rmse_r$ and $rmse_z$. The value of *Emax* is approximately 2·6 times that of the corresponding rmse, both in vertical and in horizontal accuracy.

An rmse of around 75 mm in *X*, *Y* and *Z* is obtained in the ZI projects. Daniel and Tennant (2001) suggest that the typical DEM accuracy generated by DPW is an $rmse_z$ of $H/9000$ and a maximum error of $3 \times rmse_z$ where *H* is the flying height above the mean terrain. In the present case, with a flying height of approximately 760 m, a theoretical vertical rmse of 84 mm and

Emax of 253 mm are obtained. These theoretical values are slightly larger than the 71·6 and 186·5 mm obtained in the study for the ZI projects with 24 control points.

In CRPS, the desired precision P is related, among other things, to the size of the individual pixels in the object space d_0, so that approximately $P \approx d_0$. In the photogrammetric projects carried out with CRPS and with 24 control points, the $rmse_r$ ranged from $1{\cdot}2 \times d_0$ to $2{\cdot}1 \times d_0$, and the $rmse_z$ from $1{\cdot}5 \times d_0$ to $2{\cdot}5 \times d_0$.

In a previous study, Mills et al. (2001) obtained $rmse_z$ values of $1{\cdot}25 \times d_0$ and $1{\cdot}05 \times d_0$ for 55 check points measured with two different close range photogrammetric software packages. The photogrammetric network was formed by three images (two models) with a pixel size on the photographed object of 1·1 mm. Lane et al. (2001) reported an $rmse_z$ of $2{\cdot}5 \times d_0$ working with vertical photographs using a Kodak DCS460 digital camera with a pixel size on the object of 0·6 mm. On the other hand, with the same camera and when a simple convergent stereopair was acquired, Chandler et al. (2005) generated DEMs with a standard deviation of 0·4 mm ($1{\cdot}20 \times d_0$). When convergent photographs were used, values for $rmse_z$ of approximately $0{\cdot}33 \times d_0$ were obtained by Pappa et al. (2001) for 521 check points, using a Kodak DC290 consumer digital camera and the Photomodeler Pro software package. With the same software and a Fujifilm MX-2900 digital camera, Fedak (2001) obtained values for rmse in X, Y and Z ranging from 0·33 to 0·75 pixels in 54 check points. An $rmse_z$ of $0{\cdot}60 \times d_0$ was reported by Aguilar et al. (2005) using ShapeCapture and three convergent photographs.

Number of Control Points

The general analysis of variance for $rmse_r$ (Table VII) and $rmse_z$ shows that the two variation sources analysed (photogrammetric project and number of ground points) are significant at the 0·05 level, whilst the interaction of both variation sources does not prove to be significant. Therefore, the results obtained with 24 well-distributed ground control points for the photogrammetric projects carried out with CRPS are much better than those generated with only 12 control points. Working with an off-the-shelf digital close range photogrammetric software package similar to that used in the present work, Deng and Faig (2001) proposed 20 to 25 control points to orient a photogrammetric network for scanned hard-copy images. In other close range photogrammetry studies, the control points were provided by 25 to 30 patterned targets placed on the model surface (Fraser and Riedel, 2000; Brasington and Smart, 2003).

Quantitative Analysis of the Errors

From this analysis, it is clear that there are three types of error in addition to those in the projects carried out with the sophisticated DPW: the error due to the use of a low-cost close range software package (CRE), the error due to the consumer-grade scanner used (SE) and the error due to the loss of resolution in the photographs (RE). These errors can be quantified by

TABLE VII. Analysis of variance table for horizontal root mean square error ($rmse_r$).

Source	*Degrees of freedom*	*Sum of squares*	*Mean square*	*F*	*Probability*
Number of control points (A)	1	15 466	15 466	10·43	0·002
Photogrammetric project (B)	6	158 112	26 352	17·77	$p < 0{\cdot}001$
Interaction (A × B)	6	4449	741	0·5	0·804
Residual	42	62 267	1482		
Total	55	240 294			

the difference in the *$rmse_r$* and *$rmse_z$* obtained between certain projects ($ZI - CR_0 = CRE$, $CR_0 - CR_1 = SE$, $CR_1 - CR_5 = RE$). The use of CRPS for conventional aerial photography as opposed to the use of DPW and 24 ground control points causes a decrease in horizontal precision of 55% and of 167% in vertical precision. The use of the flatbed HP scanner as opposed to that of a photogrammetric scanner causes a decrease in accuracy of 29% in horizontal and 42% in vertical precision. Finally, the use of 42 µm per pixel resolutions as opposed to that of 20 µm per pixel resolutions generates an increase in error of 21% and 18% in horizontal and vertical precision, respectively.

On the other hand, the cost of a close range software package is around €1500, whereas the basic software of a DPW can cost around €30 000. In addition, the increase in error due to the use of a consumer-grade scanner can be reduced by photogrammetric calibration (Sampson et al., 1999).

Applications and Planimetric Scale

The methodology described based on the use of CRPS with aerial photographs makes it possible for engineering firms to construct their own large-scale maps of small areas at the lowest possible cost. These maps can be used in various fields such as geographical information systems (GIS), forestry, soil science, environmental monitoring, urban and rural development, and most important of all, they are produced by the engineers themselves who are also going to be the users, and would thus be able to have tailor-made maps for their specific requirements. In order to keep costs to a minimum, it would be necessary to obtain low-cost access to aerial photographs from the numerous flights carried out by government agencies. Before importing the images into the CRPS, it is necessary to split the area of interest within the pair of photographs or resample the original images to a lower resolution, so that the size of the files is reduced and they can be loaded onto the CRPS. The principal problem of the low-cost method proposed compared to the DPW, besides the loss of precision already mentioned in obtaining the coordinates, is the relative lack of automation of the photogrammetric processes and of the measurement of points, which increases the working time considerably in the CRPS, so that it would only be applicable to small areas. Moreover, the CRPS does not have modules at its disposal to generate DEM automatically, and would therefore be mainly appropriate for the generation of planimetric maps.

Bearing these considerations in mind, from a photogrammetric flight that allows planimetric maps at a scale of 1:1000 using DPW to be obtained, the accuracy in measuring survey points with CRPS allows planimetric maps to be generated at scales ranging from 1:1500 for CR_0 to 1:2500 for CR_5 (Fig. 4).

CONCLUSIONS

In these experiments, the application of a low-cost close range software package for the measurement of coordinates of points on the land surface was shown to enable users to obtain planimetric and vertical root mean square errors of 164·4 and 191·3 mm with photogrammetric scanners and 24 control points, using conventional aerial photographs at a scale of 1:5000. These errors, although higher than those resulting from the use of sophisticated and expensive digital photogrammetric stations, allow the generation of planimetric maps at a scale of 1:1500 and topographic maps with a contour interval of around 1 m. This methodology is of great interest to small engineering firms for the generation of local area maps.

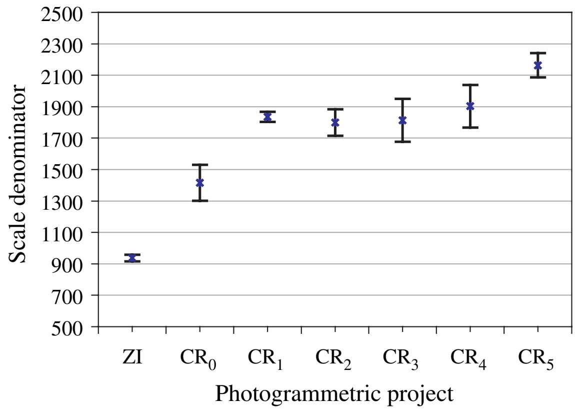

FIG. 4. Scale denominator for 24 ground control points; error bars at 95% confidence level. This figure appears in colour in the electronic version of the article and in the plate section at the front of the printed journal

The decrease in precision of the measurement of coordinates using close range photogrammetric systems as opposed to digital photogrammetric workstations for 24 ground control points was 55% in the horizontal and 167% in the vertical. The use of the HP Scanjet 5400C consumer-grade scanner versus that of the Vexcel UltraScan 5000 photogrammetric scanner lowered precision by 29% in the horizontal and 42% in the vertical, whilst the use of 42 µm per pixel resolutions as opposed to that of 20 µm per pixel resolutions generated an increase in error of 21% and 18% in horizontal and vertical precisions, respectively.

The main drawbacks of the close range photogrammetry software used in this study are the following:

(1) The impossibility of importing high resolution full-size aerial digital images at a scale of 1:5000, which in TIFF format take up around 392 Mb.
(2) The search for homologous points in each of the images is done both monoscopically and manually.
(3) The absence of a module for the automatic generation of DEMs limits its use for producing topographic maps with contours. This disadvantage might be overcome by using slightly more expensive digital photogrammetry software including automatic DEM extraction by image matching (for example, PI-3000 from Topcon).
(4) The vast number of control points necessary for the calibration and registration of images (24 ground control points) requires major fieldwork support.

However, the results obtained in this study are encouraging and show the possibility of measuring terrain coordinates from a conventional aerial photography with low-cost methods, although logically the precisions obtained and the lack of automation limit their use to the planimetric mapping of small areas.

ACKNOWLEDGEMENTS

The authors greatly appreciate the cooperation of D.a.p. (State-owned Company of the Agrarian and Fishing Development of Andalusia, Spain) for all their assistance and for the opportunity to use their 1:5000 scale aerial photography of Níjar (Almería).

REFERENCES

AGUILAR, M. A., AGUILAR, F. J., AGÜERA, F. and CARVAJAL, F., 2005. The evaluation of close-range photogrammetry for the modelling of mouldboard plough surfaces. *Biosystems Engineering*, 90(4): 397–407.

BAILY, B., COLLIER, P., FARRES, P., INKPEN, R. and PEARSON, A., 2003. Comparative assessment of analytical and digital photogrammetric methods in the construction of DEMs of geomorphological forms. *Earth Surface Processes and Landforms*, 28(3): 307–320.

BRASINGTON, J. and SMART, R. M. A., 2003. Close range digital photogrammetric analysis of experimental drainage basin evolution. *Earth Surface Processes and Landforms*, 28(3): 231–247.

CHANDLER, J. H., FRYER, J. G. and JACK, A., 2005. Metric capabilities of low-cost digital cameras for close range surface measurement. *Photogrammetric Record*, 20(109): 12–26.

DANIEL, C. and TENNANT, K., 2001. DEM quality assessment. *Digital Elevation Model Technologies and Applications: The DEM Users Manual* (Ed. D. F. Maune). American Society for Photogrammetry and Remote Sensing, Bethesda, Maryland. 539 pages: 395–440.

DENG, G. and FAIG, W., 2001. An evaluation of an off-the-shelf digital close-range photogrammetric software package. *Photogrammetric Engineering & Remote Sensing*, 67(2): 227–233.

FEDAK, M., 2001. 3D measurement accuracy of a consumer-grade digital camera and retro-reflexive survey targets. Eos Systems Inc., Vancouver, British Columbia. http://www.photomodeler.com/pmpro07.html [Accessed 21st January 2005].

FGDC, 1998. Geospatial Positioning Accuracy Standard, Part 3: National Standard for Spatial Data Accuracy. Federal Geographic Data Committee, c/o USGS, Reston, Virginia. http://www.fgdc.gov/standards/documents/standards/accuracy/chapter3.pdf [Accessed 22nd November 2004].

FRASER, C. S., 1993. A resumé of some industrial applications of photogrammetry. *ISPRS Journal of Photogrammetry and Remote Sensing*, 48(3): 12–23.

FRASER, C. S., 1994. Large scale mapping from small format imagery. *International Archives of Photogrammetry and Remote Sensing*, 30(4): 332–337.

FRASER, C. S., 1997. Digital camera self-calibration. *ISPRS Journal of Photogrammetry and Remote Sensing*, 52(4): 149–159.

FRASER, C. S. and RIEDEL, B., 2000. Monitoring the thermal deformation of steel beams via vision metrology. *ISPRS Journal of Photogrammetry and Remote Sensing*, 55(4): 268–276.

GOOCH, M. J., CHANDLER, J. H. and STOJIC, M., 1999. Accuracy assessment of digital elevation models generated using the Erdas Imagine OrthoMAX digital photogrammetric system. *Photogrammetric Record*, 16(93): 519–531.

GRANSHAW, S. I., 1980. Bundle adjustment methods in engineering photogrammetry. *Photogrammetric Record*, 10(56): 181–207.

GREEN, J., MATTHEWS, S. and TURANLI, T., 2002. Underwater archaeological surveying using PhotoModeler, Virtualmapper: different applications for different problems. *International Journal of Nautical Archaeology*, 31(2): 283–292.

GRUBER, M. and LEBERL, F., 2001. Description and evaluation of the high quality photogrammetric scanner UltraScan 5000. *ISPRS Journal of Photogrammetry and Remote Sensing*, 55(5/6): 313–329.

HERITAGE, G. L., FULLER, I. C., CHARLTON, M. E., BREWER, P. A. and PASSMORE, D. P., 1998. CDW photogrammetry of low relief fluvial features: accuracy and implications for reach-scale sediment budgeting. *Earth Surface Processes and Landforms*, 23(13): 1219–1233.

KENEFICK, J. F., GYER, M. S. and HARP, B. F., 1972. Analytical self-calibration. *Photogrammetric Engineering*, 38(11): 1117–1126.

LANE, S. N., CHANDLER, J. H. and PORFIRI, K., 2001. Monitoring river channel and flume surfaces with digital photogrammetry. *Journal of Hydraulic Engineering*, 127(10): 871–877.

MAAS, H.-G., VIRANT, M., BECKER, J., BÖSEMANN, W., GATTI, L. and HENRICHS, A., 2002. Photogrammetric methods for measurements in fluid physics experiments in space. *Acta Astronautica*, 50(4): 225–231.

MASON, S., RÜTHER, H. and SMIT, J., 1997. Investigation of the Kodak DCS460 digital camera for small-area mapping. *ISPRS Journal of Photogrammetry and Remote Sensing*, 52(5): 202–214.

MILLS, J. P., NEWTON, I. and GRAHAM, R. W., 1996. Aerial photography for survey purposes with a high resolution, small format, digital camera. *Photogrammetric Record*, 15(88): 575–587.

MILLS, J. P., NEWTON, I. and PEIRSON, G. C., 2001. Pavement deformation monitoring in a rolling load facility. *Photogrammetric Record*, 17(97): 7–24.

MILLS, J. P. and BARBER, D., 2004. Geomatics techniques for structural surveying. *ASCE Journal of Surveying Engineering*, 130(2): 56–64.

PAPPA, R. S., GIERSCH, L. R. and QUAGLIAROLI, J. M., 2001. Photogrammetry of a 5 m inflatable space antenna with consumer-grade digital cameras. *Experimental Techniques*, 25(4): 21–29.

SAMPSON, R. D., PETERSON, A. E. and LOZOWSKI, E. P., 1999. Photogrammetric calibration of a consumer grade flat-bed scanner. *Proceedings of the IEEE Canadian Conference on Electrical and Computer Engineering*, Shaw Conference Center, Edmonton. Vol. 2. 718 pages: 622–626.

SMITH, M. J. and SMITH, D. G., 1996. Operational experiences of digital photogrammetric systems. *International Archives of Photogrammetry and Remote Sensing*, 31(B2): 357–362.

SNEDECOR, G. W. and COCHRAN, W. G., 1980. *Statistical Methods*. Seventh edition. Iowa State University Press, Ames, Iowa. 507 pages.

WALKER, A. S., 1995. Analogue, analytical and digital photogrammetric workstations: practical investigations of performance. *Photogrammetric Record*, 15(85): 17–25.

Résumé

Produire des cartes sur des petites surfaces en utilisant des photographies aériennes conventionnelles est d'un grand intérêt pour les petites sociétés d'ingénierie. Le problème principal est le coût élevé des stations de travail utilisées pour la photogrammétrie numérique. Dans cet article, on montre l'utilisation d'un logiciel de photogrammétrie à bas prix pour la mesure de points 3D à partir d'un vol à l'échelle approximative du 1:5000. De plus, nous étudions l'influence du type de scanner utilisé pour numériser les images (scanner de bureau ou scanner photogrammétrique), la résolution des images scannées et le nombre de points d'appui nécessaires. Les erreurs RMS obtenues sur les points de contrôle avec un logiciel photogrammétrique à bas prix, un scanner photogrammétrique et 24 points d'appui, sont d'environ 116 mm en XY et 191 mm en Z. Un tel niveau de précision permet la production de plans à l'échelle du 1:5000 et de cartes topographiques avec une équidistance des courbes de niveau d'environ 1 m. Avec un scanner de bureau, l'erreur RMS devient d'environ 150 mm en XY et 271 mm en Z.

Zusammenfassung

Für Ingenieurbüros ist die Möglichkeit der Kartierung kleiner Gebiete mittels traditioneller Luftbildphotogrammetrie von großem Interesse. Allerdings stehen dem die hohen Kosten für leistungsfähige digitale photogrammetrische Arbeitsstationen gegenüber. Als Alternative wird hier ein kostengünstiges photogrammetrisches Softwarepaket für Nahbereichsanwendungen für die dreidimensionale Auswertung eines photogrammetrischen Luftbildblockes mit Bildmaßstab 1:5000 eingesetzt. Neben der Anwendbarkeit werden die Einflüsse des Scanners (Desktop- oder photogrammetrischer Scanner), der Auflösung der digitalen Bilder und der Anzahl der notwendigen Passpunkte untersucht. Die mittleren quadratischen Fehler an den Kontrollpunkten lagen bei der Anwendung eines photogrammetrischen Scanners und 24 Passpunkten bei ungefähr 116 mm für X und Y Koordinaten, und bei 191 mm für Z. Damit können Grundrisse im Maßstab 1:1500 und topographische Karten mit einem Höhenlinienintervall von ca. 1 m hergestellt werden. Im Vergleich dazu lagen bei Verwendung eines Desktopscanners die mittleren quadratischen Fehler bei ca. 150 mm für X und Y, und 271 mm für Z.

Resumen

La posibilidad de generar planos de superficies pequeñas utilizando fotografía aérea convencional es de gran interés para pequeños gabinetes de ingeniería. El principal problema es el alto coste económico de las sofisticadas estaciones *fotogramétricas digitales con las que usualmente se realizan. En este artículo, se utiliza un programa de fotogrametría de objeto cercano y bajo coste para obtener las coordenadas tridimensionales de puntos sobre la superficie del terreno, a partir de un vuelo aéreo a una escala aproximada de 1:5000. Además, se estudia la influencia del tipo de escáner empleado en la digitalización de los fotogramas (escáner de oficina o escáner fotogramétrico), la resolución de las imágenes digitales y el número de puntos de control requeridos. El error medio cuadrático obtenido en los puntos de comprobación, cuando usamos el programa de fotogrametría de objeto cercano y bajo coste, un escáner fotogramétrico y 24 puntos de control, estuvo en torno a los 116 mm en X e Y, y 191 mm para la coordenada Z. Estos niveles de exactitud permiten la generación de planos planimétricos a escala 1:1500 y topográficos con una equidistancia entre curvas de nivel de exactitud de 1 m. Cuando empleamos un escáner de oficina para la digitalización de las imágenes, el error medio cuadrático fue de unos 150 mm en X e Y, y 271 mm en Z.*

